Cell Reports, Volume *7*

Supplemental Information

Targeting Polycomb to Pericentric Heterochromatin in Embryonic Stem Cells Reveals a Role for H2AK119u1 in PRC2 Recruitment

Sarah Cooper, Martin Dienstbier, Raihann Hassan, Lothar Schermelleh, Jafar Sharif, Neil P. Blackledge, Valeria De Marco, Sarah Elderkin, Haruhiko Koseki, Robert Klose, Andreas Heger, and Neil Brockdorff

Figure S1

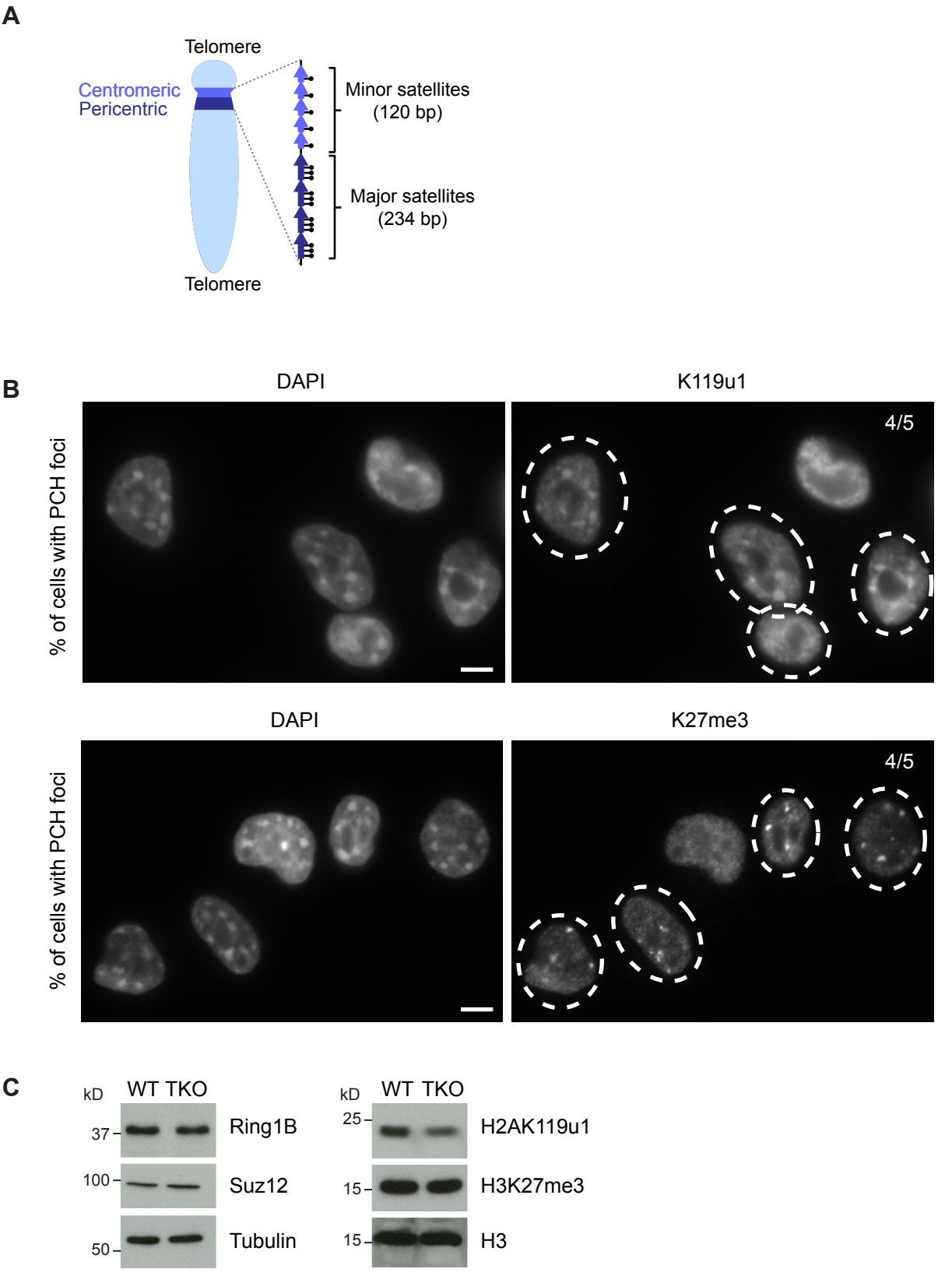
A
Telomere
Centromeric
Pericentric
Minor satellites
(120 bp)
Major satellites
(234 bp)
Telomere
B
DAPI
K119u1
4/5
% of cells with PCH foci
DAPI
K27me3
4/5
% of cells with PCH foci
C
kD
WT TKO
37
Ring1B
100
Suz12
50
Tubulin
kD
WT TKO
25
H2AK119u1
15
H3K27me3
15
H3

Figure S2

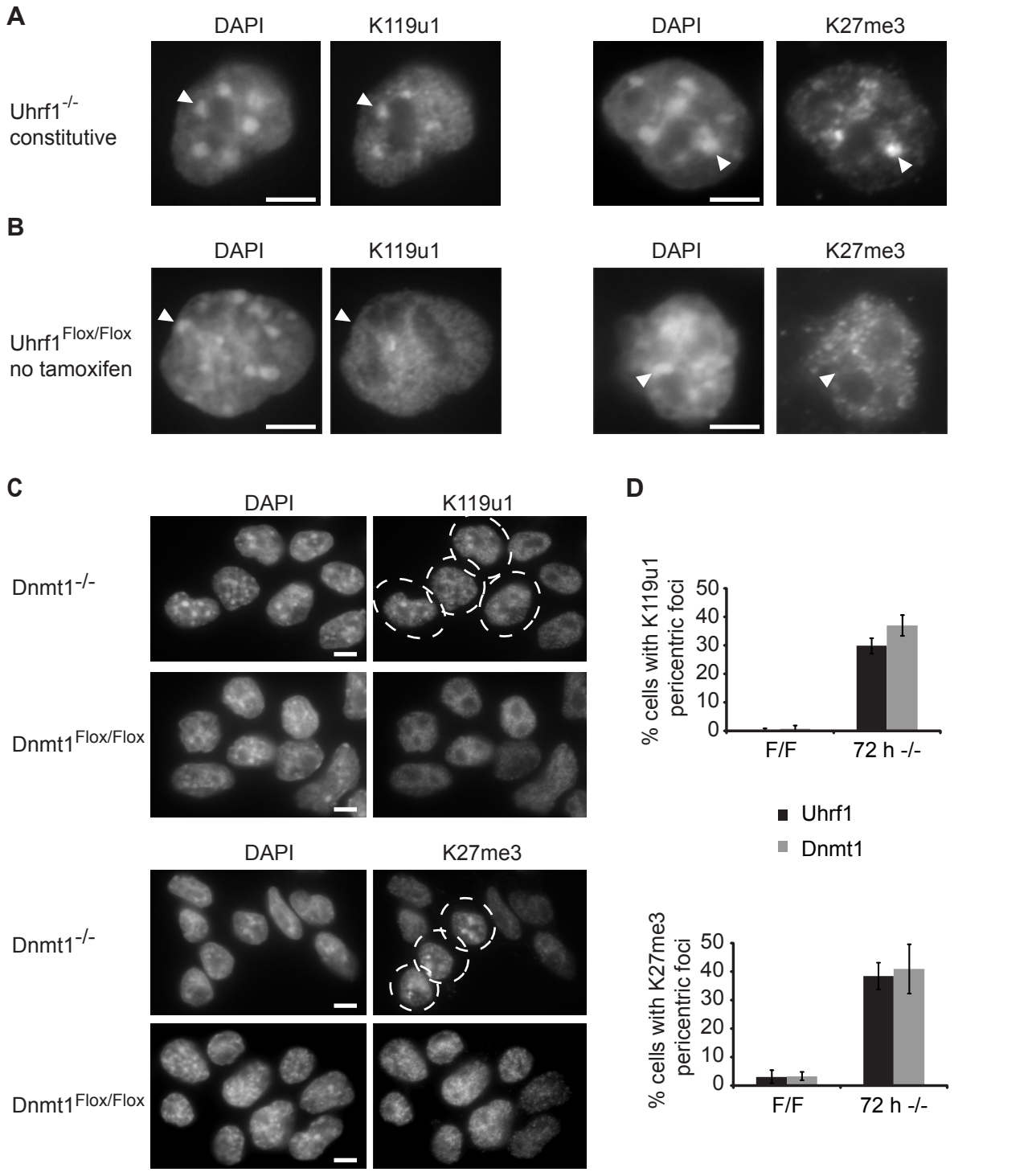
A
DAPI
K119u1
DAPI
K27me3
Uhrf1-/-
constitutive
B
DAPI
K119u1
DAPI
K27me3
Uhrf1Flox/Flox
no tamoxifen
C
DAPI
K119u1
Dnmt1-/-
Dnmt1Flox/Flox
DAPI
K27me3
Dnmt1-/-
Dnmt1Flox/Flox
D
% cells with K119u1 pericentric foci
50
40
30
20
10
0
F/F
72 h -/-
Uhrf1
Dnmt1
% cells with K27me3 pericentric foci
50
40
30
20
10
0
F/F
72 h -/-

Figure S3

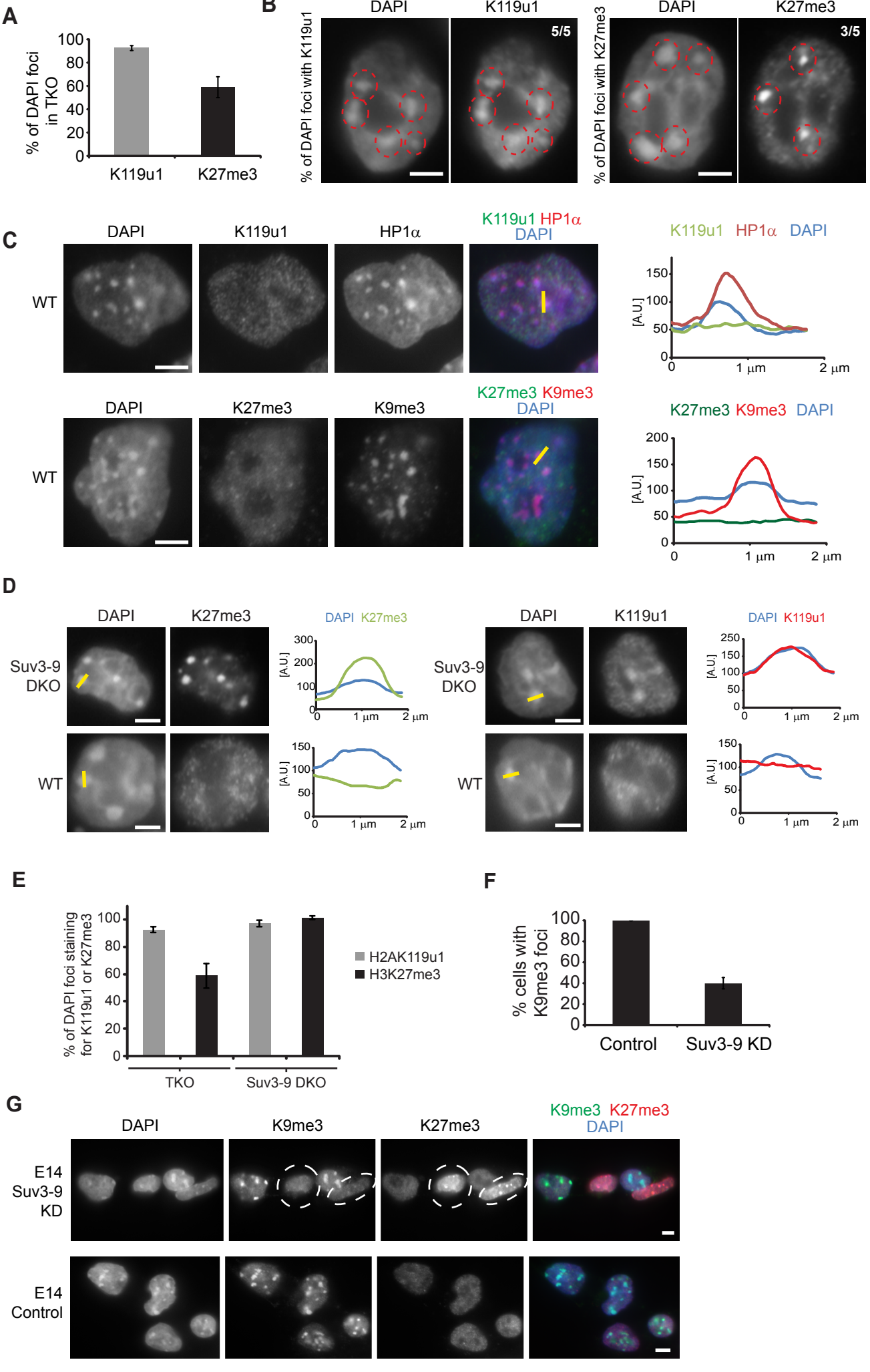
A
% of DAPI foci in TKO
100
80
60
40
20
0
K119u1
K27me3
B
DAPI
K119u1
% of DAPI foci with K119u1
5/5
DAPI
K27me3
% of DAPI foci with K27me3
3/5
C
DAPI
K119u1
HP1α
K119u1 HP1α DAPI
WT
K119u1 HP1α DAPI
[A.U.]
150
100
50
0
0
1 μm
2 μm
DAPI
K27me3
K9me3
K27me3 K9me3 DAPI
WT
K27me3 K9me3 DAPI
[A.U.]
200
150
100
50
0
0
1 μm
2 μm
D
DAPI
K27me3
DAPI K27me3
Suv3-9 DKO
WT
[A.U.]
300
200
100
0
150
100
50
0
0
1 μm
2 μm
DAPI
K119u1
DAPI K119u1
Suv3-9 DKO
WT
[A.U.]
250
150
100
50
0
150
100
50
0
0
1 μm
2 μm
E
% of DAPI foci staining for K119u1 or K27me3
100
80
60
40
20
0
H2AK119u1
H3K27me3
TKO
Suv3-9 DKO
F
% cells with K9me3 foci
100
80
60
40
20
0
Control
Suv3-9 KD
G
DAPI
K9me3
K27me3
K9me3 K27me3 DAPI
E14 Suv3-9 KD
E14 Control

Figure S4

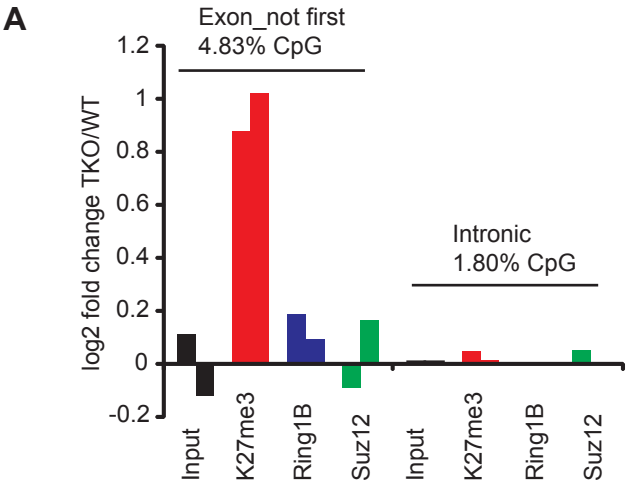
A
Exon_not first
4.83% CpG
Intronic
1.80% CpG
log2 fold change TKO/WT
1.2
1
0.8
0.6
0.4
0.2
0
-0.2
Input
K27me3
Ring1B
Suz12
Input
K27me3
Ring1B
Suz12

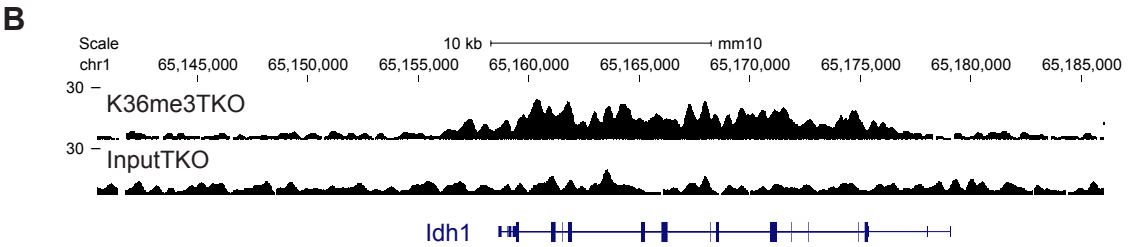
B
Scale
chr1
10 kb
mm10
65,145,000
65,150,000
65,155,000
65,160,000
65,165,000
65,170,000
65,175,000
65,180,000
65,185,000
30
K36me3TKO
30
InputTKO
Idh1

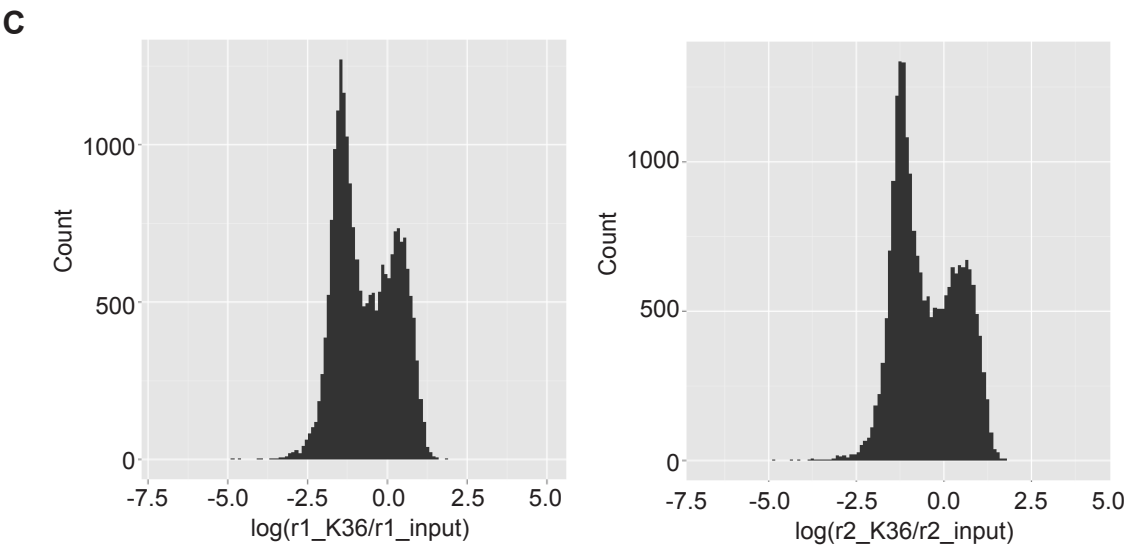
C
Count
1000
500
0
-7.5
-5.0
-2.5
0.0
2.5
5.0
log(r1_K36/r1_input)
Count
1000
500
0
-7.5
-5.0
-2.5
0.0
2.5
5.0
log(r2_K36/r2_input)

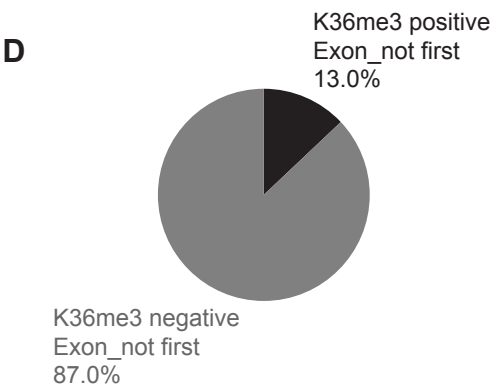
D
K36me3 positive
Exon_not first
13.0%
K36me3 negative
Exon_not first
87.0%

Figure S5

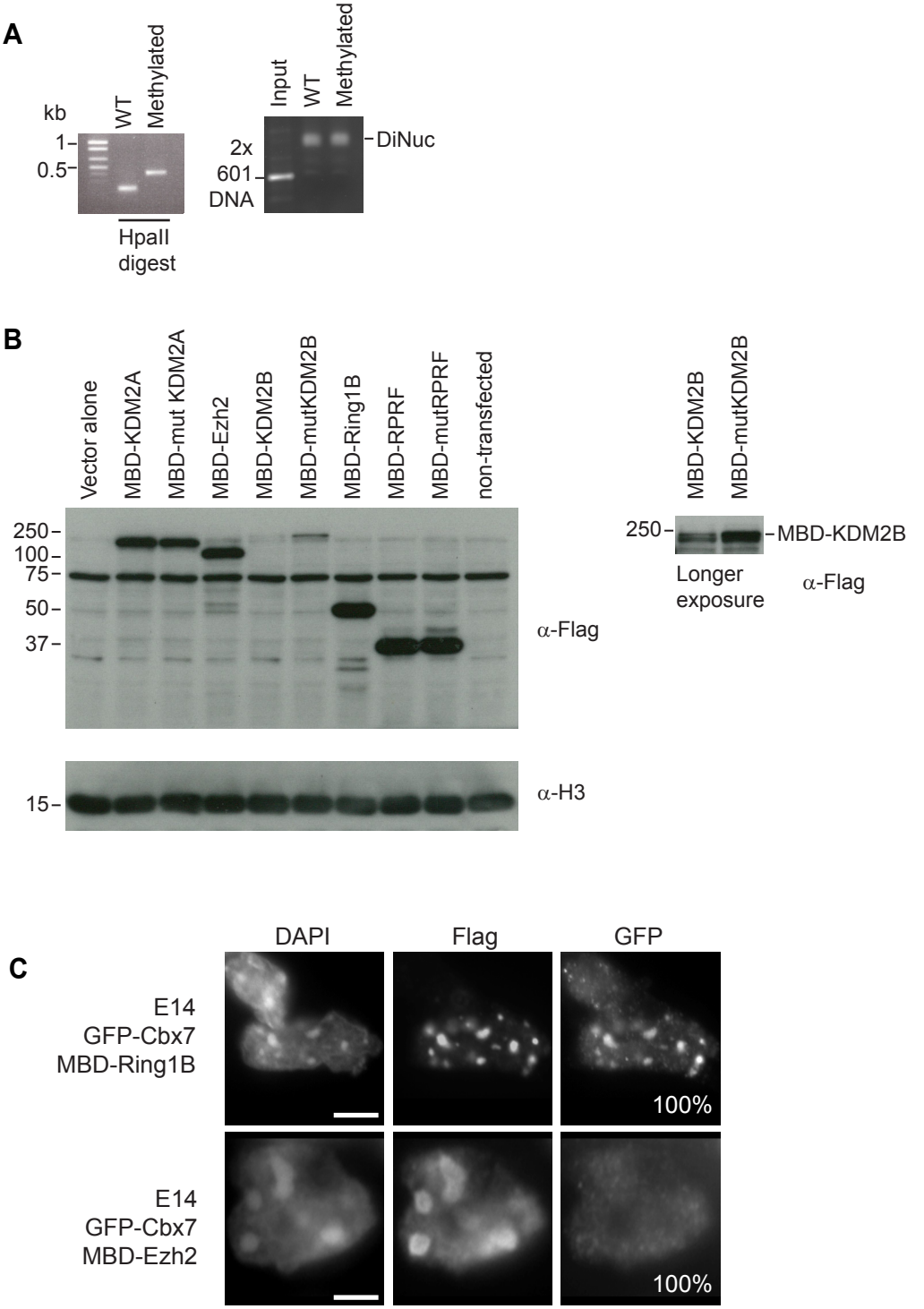
A
kb
WT
Methylated
1
0.5
HpaII digest
Input
WT
Methylated
2x 601 DNA
DiNuc
B
Vector alone
MBD-KDM2A
MBD-mut KDM2A
MBD-Ezh2
MBD-KDM2B
MBD-mutKDM2B
MBD-Ring1B
MBD-RPRF
MBD-mutRPRF
non-transfected
250
100
75
50
37
α-Flag
15
α-H3
MBD-KDM2B
MBD-mutKDM2B
250
MBD-KDM2B
Longer exposure
α-Flag
C
DAPI
Flag
GFP
E14
GFP-Cbx7
MBD-Ring1B
100%
E14
GFP-Cbx7
MBD-Ezh2
100%

Figure S6

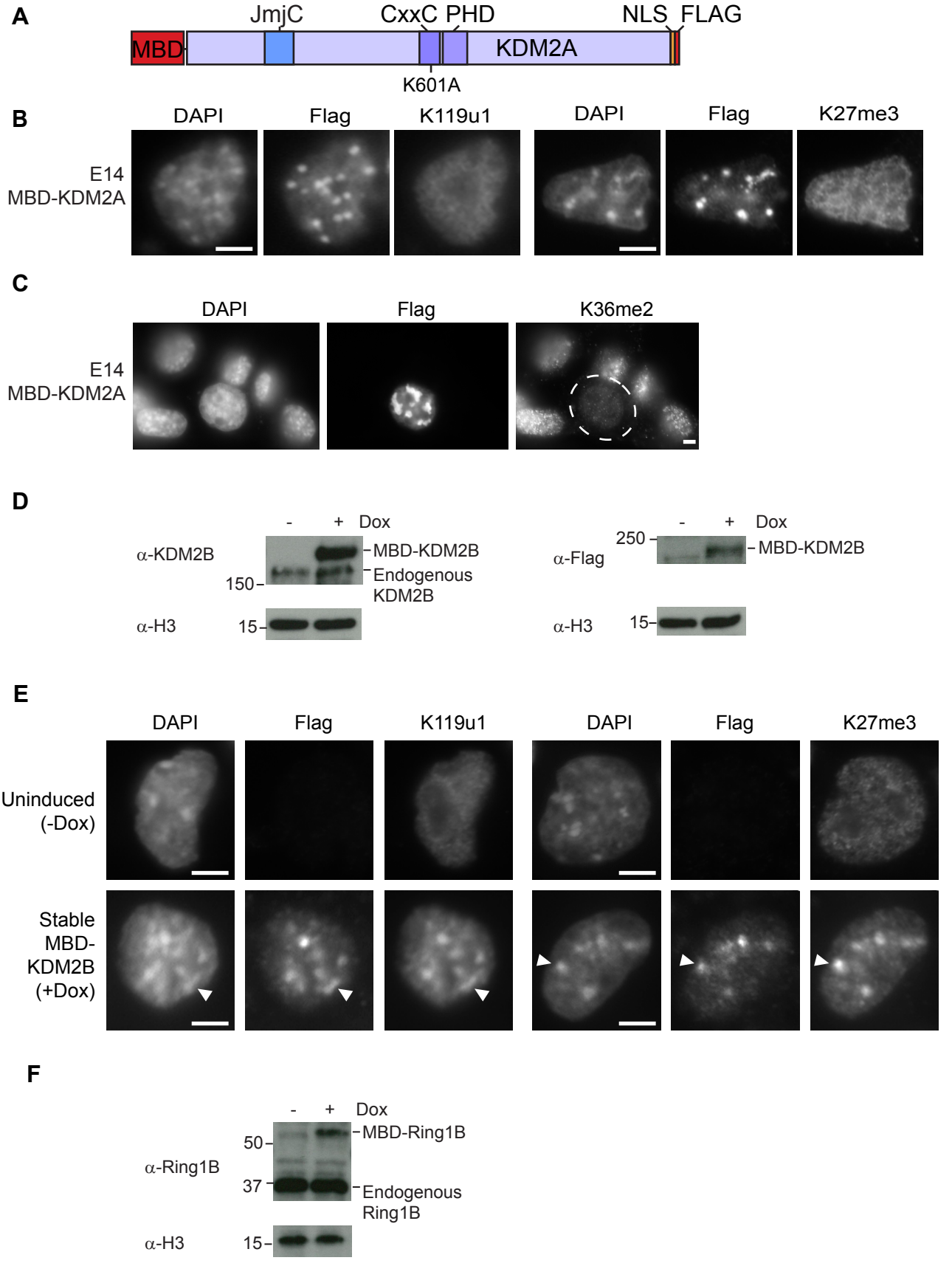
A
JmjC
CxxC PHD
NLS FLAG
MBD
KDM2A
K601A
B
DAPI
Flag
K119u1
DAPI
Flag
K27me3
E14
MBD-KDM2A
C
DAPI
Flag
K36me2
E14
MBD-KDM2A
D
- + Dox
α-KDM2B
MBD-KDM2B
150
Endogenous
KDM2B
α-H3
15
- + Dox
250
α-Flag
MBD-KDM2B
α-H3
15
E
DAPI
Flag
K119u1
DAPI
Flag
K27me3
Uninduced
(-Dox)
Stable
MBD-
KDM2B
(+Dox)
F
- + Dox
50
α-Ring1B
MBD-Ring1B
37
Endogenous
Ring1B
α-H3
15

Figure S7

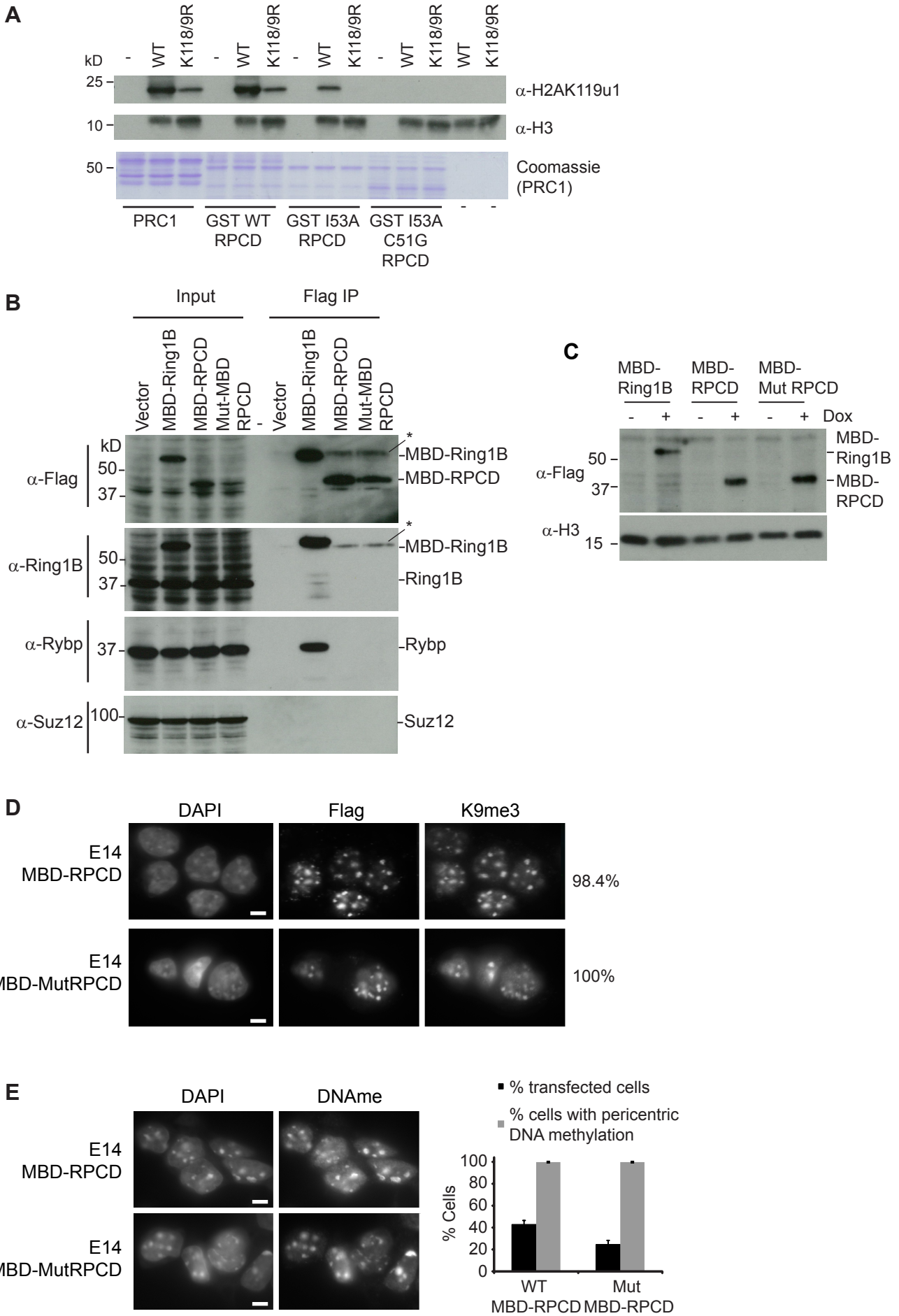
A
kD
-
WT
K118/9R
25
10
50
α-H2AK119u1
α-H3
Coomassie (PRC1)
PRC1
GST WT RPCD
GST I53A RPCD
GST I53A C51G RPCD
B
Input
Flag IP
Vector
MBD-Ring1B
MBD-RPCD
Mut-MBD RPCD
α-Flag
α-Ring1B
α-Rybp
α-Suz12
100
MBD-Ring1B
MBD-RPCD
Ring1B
Rybp
Suz12
C
MBD-Ring1B
MBD-RPCD
MBD-Mut RPCD
Dox
α-H3
15
D
DAPI
Flag
K9me3
E14 MBD-RPCD
E14 MBD-MutRPCD
98.4%
100%
E
DAPI
DNAme
% transfected cells
% cells with pericentric DNA methylation
% Cells
WT MBD-RPCD
Mut MBD-RPCD

Supplemental Figure Legends

Figure S1

PcG complexes localise to PCH in response to loss of DNA methylation. Related to Figure 1. A. Schematic of mouse PCH. B. IF of TKO cells stained for H2AK119u1 or H3K27me3, and DNA stained with DAPI, showing a typical field of view. Cells showing PCH foci positive for H2AK119u1 or H3K27me3 are circled in white to illustrate the scoring in Figure 1B. C. Western blot analysis of levels of PRC1 (Ring1B, H2AK119u1) and PRC2 (Suz12, H3K27me3) proteins and modifications, along with loading controls (Tubulin, histone H3), in WT and TKO cells. Scale bars 5 μm.

Figure S2

PcG complexes are dynamically acquired at PCH upon loss of DNA methylation. Related to Figure 2. A. IF of constitutive Uhrf1 $^{-/-}$ cells stained for H2AK119u1 or H3K27me3. Arrowheads indicate a single PCH domain. B. IF of WT (Uhrf $^{Flox/Flox}$) cells stained for H2AK119u1 or H3K27me3. Arrowheads indicate a single PCH domain. C. IF of Dnmt1 $^{-/-}$ (72 h, tamoxifen treatment) or WT (Dnmt1$^{Flox/Flox}$) cells stained for H2AK119u1 or H3K27me3. Cells showing PCH foci positive for H2AK119u1 or H3K27me3 are circled in white. D. Graphs to compare % of cells with H2AK119u1 or H3K27me3 foci in Uhrf1$^{-/-}$ and Dnmt1 $^{-/-}$ cells (72 h, tamoxifen treatment). Bars show average (n >200 cells) +/- SD (n=3). Scale bars 5 μm.

Figure S3

H3K9me3 antagonises PcG recruitment. Related to Figure 3. A. Graph to show % of DAPI foci staining for H2AK119u1 or H3K27me3 in TKO cells. Bars show average (n>200 DAPI foci) +/- SD (n=3). B. IF of TKO cells with DAPI foci, H2AK119u1 and H3K27me3 foci marked with red circles to illustrate scoring shown in A and Figure 3E. C. IF of WT cells co-stained for H2AK119u1 and HP1α, or H3K27me3 and H3K9me3. The graphs show a profile plot of fluorescence intensity (Arbitrary units, A.U.) across a single PCH domain (2 μM) defined by DAPI and marked on the merge image as a yellow bar. D. IF of Suv3-9h1/h2 DKO and WT cells stained for H3K27me3 (left) or H2AK119u1 (right). Graphs, as in C, show profiles of a single PCH domain marked as a yellow bar. E. Graph to show % of DAPI foci staining for H2AK119u1 (grey) or H3K27me3 (black) in TKO cells or in Suv3-9h1/h2 DKO cells. Bars show average (n>200 DAPI foci) +/- SD (n=3). F. Graph to show % cells with H3K9me3 foci in Uhrf1$^{-/-}$ cells upon Suv3-9h1/h2 knockdown. Bars show average (n >200 cells) +/- SD (n=3). G. Knockdown of Suv3-9h1/h2 or a scrambled control in E14

ESCs, co-stained for H3K27me3 and H3K9me3. White circles indicate cells with Suv3-9h1/h2 KD. Scale bars 5 µm.

Figure S4

Upon DNA methylation loss, PcG complexes are redistributed to exon sequences, defined by H3K36me3 occupancy. Related to Figure 4. A. Graph to show the fold change of reads, normalised to total reads, from ChIP-seq analysis of Input, H3K27me3, Ring1B and Suz12 in TKO relative to WT cells, at exons (excluding first exon) or introns. B. Screen shot of one biological repeat of ChIP-seq of H3K36me3 and Input in TKO cells. C. Distribution of fold change between H3K36me3 total read count and input total read count in two biological replicates. D. Pie chart to show % of exons (excluding first) which are defined as positive or negative for H3K36me3.

Figure S5. DNA methylation does not directly inhibit PcG activity in vitro or in vivo. Related to Figure 5 and 6. A. Left panel shows an agarose gel of a methylation sensitive digest (HpaII) of WT or in vitro methylated 601 positioning sequence DNA. Right panel shows EMSA analysis of reconstituted di-nucleosomes run on 0.8% agarose gel, post-stained with ethidium bromide. B. Western blot analysis, probed for Flag and H3, of whole cell extracts from E14 ESCs transiently transfected with MBD tethering constructs. Right panel shows longer exposure of same blot to highlight MBD-KDM2B constructs. C. MBD-Ring1B-Flag or MBD-Ezh2-Flag transfected into ESCs stably expressing GFP-Cbx7, stained for Flag and GFP. % of cells showing illustrated phenotype is indicated (n>100). Scale bars 5 µm.

Figure S6. KDM2B, but not KDM2A, can recruit PRC2 activity to PCH domains. Related to Figure 6. A. Schematic of MBD-KDM2A-Flag showing the position of the mutation in the CxxC domain (K-A). B. MBD-KDM2A-Flag transfected into E14 ESCs stained for H3K27me3 and H2AK119u1. C. As B, stained for Flag and H3K36me2. The white circle indicates reduction of H3K36me2 upon MBD-KDM2A expression. D. Western blot showing nuclear extracts from inducible stable MBD-KDM2B-Flag cell lines, plus or minus doxycycline, probed using an antibody against KDM2B (left) or Flag (right), and an antibody against histone H3 as a loading control. E. Inducible stable line expressing MBD-KDM2B-Flag, either non-induced or induced for 3 days with doxycycline, and stained for Flag and H2AK119u1 (left) and Flag and H3K27me3 (right). Arrowheads indicate an example of staining within Flag domains at PCH. F. Western blot showing whole cell

extracts from inducible stable MBD-Ring1B-Flag cell lines, plus or minus doxycycline, probed using an antibody against Ring1B and H3 (loading control). Scale bars 5 μm.

Figure S7. Ubiquitylated H2A is sufficient to recruit PRC2 to PCH domains. Related to Figure 7. A. PRC1 ubiquitylation assay using WT or H2AK118R/K119R nucleosomes as substrate, and analysed by western blot (probed for H2AK119u1 or H3). Recombinant PRC1 and RPCD proteins are shown by Coomassie staining (lower panel). B. Coimmunoprecipitation experiment using E14 cells transfected with empty vector, MBD-Ring1B-Flag, MBD-RPCD-Flag, or MBD-mut-RPCD-Flag and immunoprecipitated with Flag beads. Western blot analysis of Input samples and IP samples, probed for Flag, Ring1B, Rybp or Suz12 antibodies. * indicates antibody heavy chain. C. Western blot showing whole cell extracts from inducible stable MBD-Ring1B-Flag, MBD-RPCD-Flag and MBD-mut-RPCD-Flag cell lines, plus or minus doxycycline, probed using an antibody against Flag and H3 (loading control). D. MBD-RPCD-Flag or MBD-mutRPCD-Flag transfected into E14 ESCs and stained for Flag and H3K9me3. Number of transfected cells with H3K9me3 PCH domains indicated (n>200). E. MBD-RPCD-Flag or MBD-mutRPCD-Flag transfected into E14 ESCs and stained with meC antibody (DNAme). Graph shows % of transfected cells (determined by Flag staining) and % of cells with meC PCH domains. Bars show average (n> 200 cells) +/- SD (n=3). Scale bars 5 μm.

Table S1

Excel table showing fold changes in TKO cells relative to WT cells at all classes of repeat. Related to Figure 4.

Table S2

Oligonucleotide sequences. Related to Figure 3 and 4.

Name	Sequence
Nkx2.25'UTRF	GTCGCTGACCAACACAAAGACG
Nkx2.25'UTRR	TGTCGTAGAAAGGGCTCTTAAGGG
Nkx2.23'UTRF	AAAGTATGCCAACTCGGTGCCA
Nkx2.23'UTRR	GGAAGATAATCTTCTGGGCTCCCA
Dlx1 F	ATGTCTCCTTCTCCCATGTCC
Dlx1 R	ACTGCACGGAACTGATGTAGG
NanogF	CCCAGGTTTCCCAATGTGAAG
NanogR	AAAGAGTCAGACCTTGCTGCCA
Map3k1F	GGGAGGGGACACCTACAGAT
Map3k1R	TTGGGCGCTTAGTGTTTTGC
Sh3bp4F	CGGGCACATCTTCCTTCACT
Sh3bp4R	ATCCGATTTGGCTTGCAGGA
Lrrc8cF	TCTGATTGTGCACTGGGCAT
Lrrc8cR	AGTGCTGTATCCATGGAGTGT
Auts2F	GTCTCTTCGGTGCATGTCCA
Auts2R	CAGGACACGTATGGTGACCC
Suv39H1F1	CCGGGCCTTTGTACTCAGGAAAGAACTCGAGTTCTTTCCTGAGTACAAAGGCTTTTTG
Suv39H1R1	AATTCAAAAAGCCTTTGTACTCAGGAAAGAACTCGAGTTCTTTCCTGAGTACAAAGGC
Suv39H1F2	CCGGCCTGCACAAGTTTGCCTACAACTCGAGTTGTAGGCAAACTTGTGCAGGTTTTTG
Suv39H1R2	AATTCAAAAACCTGCACAAGTTTGCCTACAACTCGAGTTGTAGGCAAACTTGTGCAGG
Suv39H2F1	CCGGCGGTAGATATTTGGTGGTTAACTCGAGTTAACCACCAAATATCTACCGTTTTTG
Suv39H2R1	AATTCAAAAACGGTAGATATTTGGTGGTTAACTCGAGTTAACCACCAAATATCTACCG
Suv39H2F2	CCGGCCACCTTTGGATGTTCATGTACTCGAGTACATGAACATCCAAAGGTGGTTTTTG
Suv39H2R2	AATTCAAAAACCACCTTTGGATGTTCATGTACTCGAGTACATGAACATCCAAAGGTGG

Table S3

Number of mapped reads from ChIP-seq samples. Related to Figure 4.

			Mapped pairs		Uniquely mapped pairs	
Track	**read length**	**total**	**pairs**	**percent**	**pairs**	**percent**
TKO-H3K27me3-R1.bwa	51	51,753,880	47,801,066	92%	38,230,376	74%
TKO-H3K27me3-R2.bwa	51	52,935,084	47,437,675	90%	37,591,517	71%
TKO-Input-R1.bwa	51	79,405,963	74,102,709	93%	59,330,219	75%
TKO-Input-R2.bwa	51	108,134,176	99,082,632	92%	78,858,197	73%
TKO-H3K36me3-R1.bwa	51	51,993,486	46,469,313	89%	36,924,092	71%
TKO-H3K36me3-R2.bwa	51	51,930,671	47,289,433	91%	37,410,446	72%
TKO-Ring1B-R1.bwa	51	98,659,073	89,163,267	90%	69,934,793	71%
TKO-Ring1B-R2.bwa	51	96,352,121	88,507,254	92%	70,592,334	73%
TKO-Suz12-R1.bwa	51	98,415,365	91,717,592	93%	75,501,142	77%
TKO-Suz12-R2.bwa	51	89,195,230	81,694,305	92%	65,136,943	73%
WT-H3K27me3-R1.bwa	51	46,490,832	43,251,087	93%	36,023,542	77%
WT-H3K27me3-R2.bwa	51	48,635,176	46,107,145	95%	38,687,931	80%
WT-Input-R1.bwa	51	123,066,448	114,053,963	93%	92,277,787	75%
WT-Input-R2.bwa	51	103,255,996	94,941,273	92%	75,021,400	73%
WT-H3K36me3-R1.bwa	51	48,065,277	43,436,203	90%	35,328,149	74%
WT-H3K36me3-R2.bwa	51	53,347,488	47,411,148	89%	39,150,307	73%
WT-Ring1B-R1.bwa	51	117,134,292	105,842,041	90%	85,555,833	73%
WT-Ring1B-R2.bwa	51	104,120,041	96,667,105	93%	78,390,261	75%
WT-Suz12-R1.bwa	51	119,071,917	110,575,020	93%	89,603,897	75%
WT-Suz12-R2.bwa	51	101,715,954	94,788,697	93%	77,113,448	76%

Extended Experimental Procedures

Cells

ESCs were grown in ES media (Dulbecco's Modified Eagle Medium (DMEM, Life Technologies) supplemented with 10% foetal calf serum (FCS, Seralab), 2 mM L-glutamine, 1x non-essential amino acids, 50 μM 2-mercaptoethanol, 50 μg/ml penicillin/streptomycin (Invitrogen) and LIF-conditioned medium, made in house, at a concentration equivalent to 1000 U/ml. Feederless ESCs were grown on tissue culture dishes coated with PBS+1% gelatine, and feeder-dependent ESCs were grown on mitomycin inactivated primary embryonic fibroblasts (PEFs). Mouse embryonic fibroblasts (MEFs) were grown in EC10 medium (DMEM, supplemented with 10% FCS, 2 mM L-glutamine, 1x non-essential amino acids, 50 μM 2-mercaptoethanol and 50 μg/ml penicillin/streptomycin).

The following cell lines were used in this study : E14TG2A, TKO ($Dnmt1^{-/-}$, $Dnmt3a^{-/-}$, $Dnmt3b^{-/-}$) and matched WT (J1) ESCs (Tsumura et al., 2006), 293 cells, conditional $Uhrf1^{-/-}$, $Dnmt1^{-/-}$ and matched WT (E14) ESCs (Sharif et al., 2007), Suv3-9h1/h2 DKO, and matched WT (E14) ESCs (Peters et al., 2003). Conditional Uhrf1 and Dnmt1 knockout cells were grown on inactivated PEFs and gene deletion was carried out by the addition of 800 nM 4-hydroxytamoxifen.

Stable clonal GFP-Cbx7 ESC lines were produced by transfecting GFP-Cbx7 in pCAG-IP (gift from Ian Chambers) into 129/1 feeder dependent ESCs and puromycin selection. Inducible, stable, clonal MBD-KDM2B, MBD-Ring1B, MBD-RPCD and MBD-mutRPCD lines were produced by co-transfecting MBD-fusions in pTRE-Tight (Clontech, see below) and pNeo Bluescript (that expresses neomycin resistance gene under the constitutive PGK promoter), into rtTA2A10 ESC lines (in which the rtTA gene is integrated into the Rosa26 locus, targeting construct gift from Anton Wutz) and selecting with G418. MBD-fusion protein expression was induced by addition of 1 μg/ml doxycycline for 3 days. WT MEFs, $Dnmt1^{-/-}$, $p53^{-/-}$ MEFs and matched control ($p53^{-/-}$) MEFs (Lande-Diner et al., 2007) were grown in EC10 medium. MEFs from $Dnmt1^{-/-}$, $p53^{+/+}$ embryos were unable to be cultured, suggesting that, unlike in ESCs, p53 is essential to protect MEFs from demethylation (Lande-Diner et al., 2007).

Constructs

Amino acids 1-112 of human MBD1, which include the MBD domain and endogenous NLS signal, followed by a glycine, serine rich flexible linker, were cloned to the N-terminus of the protein of interest in pBluescript. A SV40 NLS, followed by a FLAG-tag were cloned on the C-terminus of the protein of interest. These MBD-fusion proteins were then cloned into the mammalian expression plasmid pCAG, in which the MBD-fusion protein was under the control of the constitutive β-actin promoter. Full length mouse Ezh2, mouse Ring1B, and human KDM2A (K601A) and KDM2B (K643A) were targeted to methylated DNA using the MBD domain. For KDM2A/B the CxxC DNA binding domains were mutated (K601A and K643A respectively). The MBD-KDM2B, MBD-Ring1B, MBD-RPCD and MBD-mutRPCD constructs were also cloned into the pTight vector to allow doxycyline inducible expression when stably integrated into rtTA2A10 ESCs (see above).

Amino acids 1-116 of Ring1B and 3-109 of Pcgf4 (termed Ring1b Pcgf4 catalytic domain RPCD fusion) were joined using a 4x GGS flexible linker and cloned with an N-terminal GST tag in pGex-6p2 for bacterial protein expression and purification, or with an N terminal MBD domain in the pCAG vector, for expression in ESCs. Catalytic mutants were made in the JmjC domain of KDM2B (H242A, I243A, D244A), and in RPCD at Ring1B I53A to mutate the E2 interaction domain and at Pcgf4 C51G to mutate the zinc finger domain, using site-directed mutagenesis kit (Stratagene). Synthesised core PRC2 subunits (full length EZH2, EED, SUZ12 and RbAp48) were codon optimized for expression in insect cells (GeneArt) and cloned into pBAC4x-1 (Novagen) using In-fusion cloning (Clontech).

Immunofluorescence

ESCs or MEFs were split onto slides 16 h before staining at low density (without feeders). Slides were then washed in PBS, fixed with 2% formaldehyde in PBS for 15 min and permeablised with 0.4% Triton X-100 in PBS for 5 min. After washing with PBS, the slides were blocked for 30 min in 0.2% fish gelatin (Sigma) in PBS and incubated for 2 h with primary antibody (diluted in 0.2% fish gelatin, and 5% normal goat serum). Slides were washed 3 times in 0.2% fish gelatin and incubated for 2 h with Alexa-fluor conjugated secondary antibody (Life Technologies). After washing 2 times in fish gelatin, and 2 times in PBS, the slides were stained with DAPI (1 µg/ml), and mounted using mounting media (Dako).

The following primary antibodies were used for immunofluroscence : H2AK119u1 (1:500, Cell Signalling, rabbit monoclonal, 8240), H3K27me3 (1:500, Diagenode,rabbit polyclonal, pAB-069-050), H3K27me3 (1:1000, Active Motif, mouse monoclonal, 61017), Flag (1:500, Sigma M2, mouse monoclonal), H3K9me3 (1:500, Active motif, rabbit polyclonal 39161), H3K4me3 (1:500, Abcam, rabbit polyclonal, ab8580), HP1α (1:500, Millipore, mouse monoclonal MAB3584) and GFP (1:100, Santa Cruz, mouse monoclonal, sc-9996).

DNA methylation staining

Slides were fixed in 4% formaldehyde for 15 min, permeablised in 0.2% Triton X-100 for 1 h and washed in 0.05% Tween-200 in PBS 3 times. They were then treated with 4M HCl with 0.1% Triton X-100 for 10 min and neutralised with 100 mM Tris-HCl pH8.8 for 30 min. After blocking overnight in 1% BSA, 0.05% Tween-20 in PBS, the primary antibody (1:500 Eurogentec, mouse monoclonal, BI-MECY-0100) was added overnight in blocking solution. Slides were washed extensively in blocking solution, secondary antibody was added for 2 h, and slides were washed again in blocking buffer and PBS before mounting (as above).

Cell transfection

ESCs or T16 MEFs were plated in a 6 well dish 16 h before transfection in ES or EC10 media without pen/strep. One hour before transfection, the media was changed. DNA (4 µg) was mixed with 8 µl lipofectamine in Optimem media, and incubated for 20 min before adding to cells. The media was changed 6 h later, and 16 h the cells were split to a 90 mm dish. The cells were split the next day to slides and fixed for immunofluorescence the following day (3 days after the initial transfection).

Quantification of PCH staining phenotypes

Slides were visualised using a 63x oil immersion objective with the Zeiss Axio Observer Z1 microscope.

Unbiased quantification of PCH enrichment

After applying a Gaussian blur filter to the images, the total nuclear area and PCH domains were defined using the Image J threshold algorithm, Triangle, based on the DAPI intensity (http://rsbweb.nih.gov/ij). The fluorescence intensity of H2AK119u1 or H3K27me3 staining

within PCH regions was then measured and expressed relative to the fluorescence intensity of the whole nucleus.

% of cells with PCH foci

The number of cells containing visible H2AK119u1 or H3K27me3 stained PCH were counted out of the total number of cells or total number of transfected cells (n>200), for three biological repeats. Error bars show standard deviation of biological repeats.

% DAPI foci

In cells with visible PCH foci, the number of foci positive for H3K27me3 or H2AK119u1 were counted out of the total number of DAPI foci (n>200), for three biological repeats. Error bars show standard deviation of biological repeats.

PCH domain cross-section analysis

A 2 µm line was drawn in Image J (shown by a yellow bar) across the PCH domain as determined by DAPI staining and the profile plot of fluorescence (arbitrary units) from each channel was obtained.

Super-resolution 3D-structured illumination microscopy (3D-SIM)

3D-SIM of immunostained ESC was performed on a DeltaVision OMX V3 Blaze system (Applied Precision Imaging/GE Healthcare), equipped with 60x/1.42 NA PlanApo oil immersion objective (Olympus), and 405, 488 and 592 nm diode lasers and Edge sCMOS cameras (PCO). SI image stacks were acquired with a z-distance of 125 nm and with 15 raw SI images per plane (5 phases, 3 angles). The SI raw data sets were computationally reconstructed with channel specific measured optical transfer functions (OTFs) and Wiener filter set to 0.003 using the softWoRX 6.0 software package (Applied Precision) to result in a 2-fold improvement of both lateral and axial resolution (Schermelleh et al., 2008). The refractive indices of the immersion oil for sample acquisition and measuring OTFs from 0.1 µm diameter FluoSphere beads (Invitrogen) were carefully selected to minimise spherical aberration. Images from the different colour channels were registered with alignment parameters obtained from calibration measurements with 0.2 µm diameter TetraSpeck beads (Invitrogen) using image registration with a linear fitting model implemented SoftWoRx 6.0. For display purposes the 32-bit reconstructed datasets were rescaled using the mode value as lower threshold for each channel to cut off half of the background and then converted to 16-bit composite tif-stacks using ImageJ.

Southern blot

Genomic DNA from conditional Uhrf1 cells was digested with the methylation sensitive enzyme HpyCH41V, separated on a 1.25% agarose gel and blotted to a hybond-XL membrane. Blots were probed with a 'gamma' mouse major satellite probe (Zvetkova et al., 2005) labelled using klenow and alpha-P-32-ATP.

Protein extract

Cells were harvested, washed in PBS and lysed with SDS-loading buffer before analysis by 12% SDS PAGE and western blot. Antibodies : Suz12 (1:250, Cell signalling, 3737S), Tubulin (1:250, Cell signalling, 2144) , Ring1B (1:1000, (Atsuta et al., 2001)) , H2AK119u1 (1:1000, Cell signalling, 8240), H3K27me3 (1:1000, Diagenode, pAB -069-100), H3 (1:10000, Abcam Ab1791) and Flag (1:1000, Sigma M2 HRP conjugated).

Chromatin Immunoprecipitation

ChIP from WT or TKO cells was performed as described in Blackledge et al., 2010 using the following antibodies : H3K27me3 (Diagenode pAB -069-100), H3K36me3 (Abcam AB9050), Suz12 (Cell Signalling 3737S), Ring1B (Atsuta et al., 2001) and H2AK119u1 (Cell signalling 8240). Three biological repeats were performed for qPCR analysis and two biological repeats were performed and, along with input samples, sent for high throughput sequencing.

Briefly, 5 x 10^7 cells were fixed with 2 µM Ethylene glycol bis[succinimidylsuccinate] (ThermoScientific) for 1 h and then 1% formaldehyde for 15 min at RT. The reaction was quenched with glycine (0.125M) and nuclei prepared in LB1 (50 mM HEPES-KOH, pH 7.9, 140 mM NaCl, 1 mM EDTA-NaOH pH 8.0, 10% Glycerol, 0.5% NP-40, 0.25% Triton X-100 and 1x complete EDTA-free protease inhibitors (Roche)). Nuclei were washed in LB2 (10 mM Tris-HCl, pH8.0, 200 mM NaCl, 1 mM EDTA-NaOH pH 8.0, 0.5 mM EGTA and 1x complete EDTA-free protease inhibitors) and lysed in LB3 (10 mM Tris-HCl, pH 8, 100 mM NaCl, 1 mM EDTA-NaOH pH 8.0, 0.5 mM EGTA, 0.1% Na-Deoxycholate, 0.5% *N*-lauroylsarcosine and 1x complete EDTA-free protease inhibitors). Chromatin was sheared in a BioRuptor sonicator (Diagenode) to produce DNA fragments with a length of <1 kb. Triton X-100 was added (1% final) and cell debris cleared by centrifugation before the sample was diluted ten-fold with dilution buffer (1% Triton X-100, 2 mM EDTA-NaOH pH 8.0, 150 mM NaCl, 20 mM Tris-HCl pH 8.0 and 1x complete EDTA-free protease inhibitors).

Samples were pre-cleared and incubated with antibodies overnight at 4°C, after removal of input aliquots. Antibody complexes were collected with 30 µl BSA and tRNA blocked rProtein A Sepharose beads and were washed once with low salt buffer (0.1% SDS, 1% Triton X-100, 2 mM EDTA-NaOH pH 8.0, 150 mM NaCl, 20 mM Tris-Cl pH 8.0), high salt buffer (0.1% SDS, 1% Triton-X-100, 2 mM EDTA-NaOH pH 8.0, 150 mM NaCl, 20 mM Tris-Cl pH 8.0), LiCl buffer (0.25 M LiCl, 1% NP-40, 1% Na-Deoxycholate, 1 mM EDTA-NaOH pH 8.0, 10 mM TrisHCl pH 8.0) and twice with TE buffer. Complexes were eluted from beads by incubation with 100 µl Elution Buffer (1% SDS, 0.1 M $NaHCO_3$) first at 65°C for 5 min, and subsequently for 30 min with vortexing at 25°C. NaCl was added to a final concentration of 200 mM and cross-links were reversed overnight at 65°C. DNA was recovered after treatment with 100 µg/ml DNase-free RNase A at 42°C for 90 min and Proteinase K (0.2 mg/ml) for 1 h at 45°C using ChIP DNA Clean & concentration columns (Zymo) and eluted in 10 µl volume. Samples for qPCR analysis were diluted 10-fold and analysed using a Biorad Chromo4 real time PCR machine (see Table S2 for primer sequences).

ChIP-seq

For ChIP-seq, undiluted purified DNA concentration was quantified using the PicoGreen dsDNA Quantitation Kit (Molecular Probes) and post-sonicated to <300 bp. Around 30 ng was sent to the Oxford Genomics Centre and 5 ng was used to prepare libraries using the NEBNext DNA Library Prep Master Mix Set for Illumina. Libraries were sequenced on an Illumina HiSeq2000 50bp paired end run.

Reads were mapped to the GRCm38 Mus musculus assembly from the UCSC genome browser (mm10, (Meyer et al., 2013) using bwa version 0.5.9-r16 (Li and Durbin, 2009) with the following options: “bwa aln -l 25 -k 2 -n 2”. BWA randomly selects a single position for reads mapping to multiple locations equally well. This mapping strategy permits quantification of the number of reads falling into different repeat categories. The number of pairs sequenced, mapped and mapped uniquely are in Table S3.

To test for local fold changes in read density, we used a window-based approach. Uniquely mapping read-pairs were counted by mid-point-overlap within 1kb windows tiled over the genome. Windows with more than 100 read pairs in input data were removed. Difference in fold change was tested using DESeq (Anders and Huber, 2010) pooling samples for dispersion estimates. We accepted windows with a 10% FDR.

Genomic annotations were obtained from the UCSC genome browser (repeats) and ENSEMBL version 72 ((Flicek et al., 2013) transcript models). We defined non-methylated

islands as the union of BioCAP-seq data from mouse testes, liver and ES cells obtained from (Long et al., 2013). Reads and genomic intervals were processed with bedtools (Quinlan and Hall, 2010). CpG content was calculated with in-house scripts.

Active and inactive genes in the TKO were defined through H3K36me3 data . Genes where both replicates contained more H3K36me3 than input reads across the genomic span were defined as active and vice versa for inactive genes (Cutoff 0 log fold change) (Figure S4).

Stable Suv3-9 H1 and H2 knockdown

Production of shRNA plasmids and lentivirus packaging were performed as previously described Tavares et al., 2012. Briefly, oligos (sequences in Table S2) were annealed and cloned into the pLK01 vector. This vector, along with packaging vectors were transfected into 293 cells using calcium phosphate transfection and 48 h later the supernatant was harvested containing lentivirus packaged shRHA hairpin.

ESCs (E14 or Uhrf1$^{-/-}$) (7.5× 10^5 per well of a 6-well dish) were plated with 250 µl of each lentivirus (Suv3-9h1 and Suv3-9h2) or scrambled control and polybrene (final concentration 8 µg/ml). Selection (1.75 µg/ml puromycin) was applied 48 hours after transduction. Cells were split to slides the day before fixing for immunofluorescence (day 6 after virus infection).

Histone purification and nucleosome reconstitution

Reconstitution of nucleosomes was performed as previously described. Briefly, recombinant Xenopus histones were expressed in bacteria and purified from inclusion bodies. H3K36CC110A mutant histone was also purified and chemically methylated in vitro (Simon, 2010). Stoichiometric amounts of each core histone were incubated together under high-salt conditions, and the resulting histone octamer was purified using a Superdex 200 gel filtration column (GE Healthcare). DNA containing two repeats of the nucleosome positioning sequence (601) and 48 bp linker was amplified by PCR and purified. DNA was then methylated using Sss1 (NEB) and methylation was assayed using methylation sensitive enzyme (HpaII) digest.

Equimolar ratios of DNA (WT or methylated) and octamers (WT or H3K36me3) were mixed together in 2 M NaCl and diluted stepwise with 10 mM Tris-HCl, pH 7.5, to reach a final concentration of 100 mM NaCl. The reconstituted dinucleosomes were analysed by an

electrophoretic mobility shift assay (EMSA) using 0.8% agarose gel in 0.2% Tris-borate and post stained with ethidium bromide.

PRC2 purification and HMTase Assay

PRC2 core complex (EZH2, EED, SUZ12 and RbAp48) in pBAC4x-1 was coexpressed using baculovirus and purified from SF9 cells. *Sf9* cells were cultured in SF900 II serum free media (Invitrogen) at 28°C. In a typical preparation, 1L of *Sf9* cells at $2x10^6$ cells/ml density was infected with 3ml of high titre PRC2 virus for 48 h. Cells were consequently harvested, washed in ice cold PBS, resuspended in potassium phosphate 20mM pH 8.0, KCl 100mM, Triton X 100 0.01%, TCEP 1mM and lysed in an EmulsiFlex-C5 homogenizer (Avestin). The complex was initially purified by affinity chromatography using the Strep(II) tag engineered at the N-terminus of EZH2, then further purified by Superose 6 size exclusion chromatography (GE Healthcare) in a buffer containing potassium phosphate 20mM pH8.0, NaCl 150mM, TCEP 1mM.

PRC2 complex (0.5 µg), dinucleosomes (0.5 µg), buffer (20 mM Tris-HCl pH8.0, 4 mM EDTA, 1mM PMSF and 0.5 mM DTT) and ^{3}H SAM (2 µl) in a total of 20 µl, were incubated for 1 h at 30°C and the reaction stopped by adding SDS-loading buffer. Samples were analysed by 18% SDS-PAGE, Coomassie stained, soaked in enhance solution and dried before exposing the gel to film overnight at -80°C.

PRC1 purification and ubiquitylation assay

PRC1 complex (Ring1B, Pcgf2, and Rybp) was coexpressed using baculovirus and purified from SF9 cells as previously described Tavares et al., 2012. GST-RPCD fusion protein (WT and mutants) were purified from bacteria using the same method as Ring1B Pcgf4 complex purification (Bentley et al., 2011). Briefly, the fusion protein was expressed in bacteria overnight grown at 16°C, and purified under native conditions using glutathione sepharose.

PRC1 ubiquitylation assays were performed using 10 µg/ml UBE1 E1 (Boston Biochem), 40 µg/ml UbcH5c E2 (Enzo life Sciences), 0.1 mg/ml methylated ubiquitin (R&D Systems), 0.2 mM ATP, 0.5µg dinucleosomes and 4 µg PRC1 or 4µg GST-RPCD fusion protein in a total volume of 20 µl. Assays were incubated for 1 h at 37°C and the reaction stopped by adding SDS-loading buffer. Samples were analysed by 18% SDS-PAGE and western blotting using H2AK119u1 and H3 antibodies.

Co-immunoprecipitation

ESCs were transfected as above and harvested 3 days after transfection. Cells were lysed in (20 mM HEPES pH 7.9, 1.5 mM MgCl2, 0.1 % NP40, 0.2 mM EDTA, 350 mM NaCl, 20 % glycerol, 0.5 mM DTT, and 1x cOmplete EDTA-free protease inhibitors) and incubated with Flag M2 agarose beads (Sigma). After extensive washing, bound proteins were eluted with FLAG peptide(100 µg/ml) and elutions were analysed by 12 % SDS-PAGE and western blot using the following antibodies : Flag (1:1000, Sigma M2 HRP conjugated), Ring1B (1:1000, (Atsuta et al., 2001), Rybp (1:500, Millipore, AB3637), Suz 12 (1:250, Cell signalling, 3737S).

Supplemental References

Anders, S., and Huber, W. (2010). Differential expression analysis for sequence count data. Genome biology *11*, R106.

Atsuta, T., Fujimura, S., Moriya, H., Vidal, M., Akasaka, T., and Koseki, H. (2001). Production of monoclonal antibodies against mammalian Ring1B proteins. Hybridoma *20*, 43-46.

Bentley, M.L., Corn, J.E., Dong, K.C., Phung, Q., Cheung, T.K., and Cochran, A.G. (2011). Recognition of UbcH5c and the nucleosome by the Bmi1/Ring1b ubiquitin ligase complex. The EMBO journal *30*, 3285-3297.

Blackledge, N.P., Zhou, J.C., Tolstorukov, M.Y., Farcas, A.M., Park, P.J., and Klose, R.J. (2010). CpG islands recruit a histone H3 lysine 36 demethylase. Molecular cell *38*, 179-190.

Flicek, P., Ahmed, I., Amode, M.R., Barrell, D., Beal, K., Brent, S., Carvalho-Silva, D., Clapham, P., Coates, G., Fairley, S*., et al.* (2013). Ensembl 2013. Nucleic acids research *41*, D48-55.

Lande-Diner, L., Zhang, J., Ben-Porath, I., Amariglio, N., Keshet, I., Hecht, M., Azuara, V., Fisher, A.G., Rechavi, G., and Cedar, H. (2007). Role of DNA methylation in stable gene repression. The Journal of biological chemistry *282*, 12194-12200.

Li, H., and Durbin, R. (2009). Fast and accurate short read alignment with Burrows-Wheeler transform. Bioinformatics *25*, 1754-1760.

Long, H.K., Sims, D., Heger, A., Blackledge, N.P., Kutter, C., Wright, M.L., Grutzner, F., Odom, D.T., Patient, R., Ponting, C.P*., et al.* (2013). Epigenetic conservation at gene regulatory elements revealed by non-methylated DNA profiling in seven vertebrates. eLife *2*, e00348.

Meyer, L.R., Zweig, A.S., Hinrichs, A.S., Karolchik, D., Kuhn, R.M., Wong, M., Sloan, C.A., Rosenbloom, K.R., Roe, G., Rhead, B*., et al.* (2013). The UCSC Genome Browser database: extensions and updates 2013. Nucleic acids research *41*, D64-69.

Peters, A.H., Kubicek, S., Mechtler, K., O'Sullivan, R.J., Derijck, A.A., Perez-Burgos, L., Kohlmaier, A., Opravil, S., Tachibana, M., Shinkai, Y*., et al.* (2003). Partitioning and plasticity of repressive histone methylation states in mammalian chromatin. Molecular cell *12*, 1577-1589.

Quinlan, A.R., and Hall, I.M. (2010). BEDTools: a flexible suite of utilities for comparing genomic features. Bioinformatics *26*, 841-842.

Schermelleh, L., Carlton, P.M., Haase, S., Shao, L., Winoto, L., Kner, P., Burke, B., Cardoso, M.C., Agard, D.A., Gustafsson, M.G*., et al.* (2008). Subdiffraction multicolor imaging of the nuclear periphery with 3D structured illumination microscopy. Science *320*, 1332-1336.

Sharif, J., Muto, M., Takebayashi, S., Suetake, I., Iwamatsu, A., Endo, T.A., Shinga, J., Mizutani-Koseki, Y., Toyoda, T., Okamura, K*., et al.* (2007). The SRA protein Np95 mediates epigenetic inheritance by recruiting Dnmt1 to methylated DNA. Nature *450*, 908-912.

Simon, M.D. (2010). Installation of site-specific methylation into histones using methyl lysine analogs. Current protocols in molecular biology / edited by Frederick M Ausubel [et al] *Chapter 21*, Unit 21 18 21-10.

Tavares, L., Dimitrova, E., Oxley, D., Webster, J., Poot, R., Demmers, J., Bezstarosti, K., Taylor, S., Ura, H., Koide, H*., et al.* (2012). RYBP-PRC1 complexes mediate H2A ubiquitylation at polycomb target sites independently of PRC2 and H3K27me3. Cell *148*, 664-678.

Tsumura, A., Hayakawa, T., Kumaki, Y., Takebayashi, S., Sakaue, M., Matsuoka, C., Shimotohno, K., Ishikawa, F., Li, E., Ueda, H.R*., et al.* (2006). Maintenance of self-renewal ability of mouse embryonic stem cells in the absence of DNA methyltransferases Dnmt1, Dnmt3a and Dnmt3b. Genes to cells : devoted to molecular & cellular mechanisms *11*, 805-814.

Zvetkova, I., Apedaile, A., Ramsahoye, B., Mermoud, J.E., Crompton, L.A., John, R., Feil, R., and Brockdorff, N. (2005). Global hypomethylation of the genome in XX embryonic stem cells. Nature genetics *37*, 1274-1279.